

## Surface spin disorder and exchange-bias in hollow maghemite nanoparticles

Hafsa Khurshid, Wanfeng Li, Manh-Huong Phan, Prithish Mukherjee, George C. Hadjipanayis et al.

Citation: *Appl. Phys. Lett.* **101**, 022403 (2012); doi: 10.1063/1.4733621

View online: <http://dx.doi.org/10.1063/1.4733621>

View Table of Contents: <http://apl.aip.org/resource/1/APPLAB/v101/i2>

Published by the [American Institute of Physics](http://www.aip.org).

---

### Related Articles

Contact resistance as a probe of near-interface ferromagnetism in GaMnAs/Cu bilayers  
*Appl. Phys. Lett.* **100**, 212403 (2012)

Magnetic properties of ZnO nanoclusters  
*J. Appl. Phys.* **111**, 084321 (2012)

Mechanically tunable magnetism on graphene nanoribbon adsorbed SiO<sub>2</sub> surface  
*J. Appl. Phys.* **111**, 074317 (2012)

Surface wave resonances supported on a square array of square metallic pillars  
*Appl. Phys. Lett.* **100**, 101107 (2012)

Perpendicular magnetic anisotropy of Ni/Cu(001) films with surface passivation  
*J. Appl. Phys.* **111**, 07C113 (2012)

---

### Additional information on *Appl. Phys. Lett.*

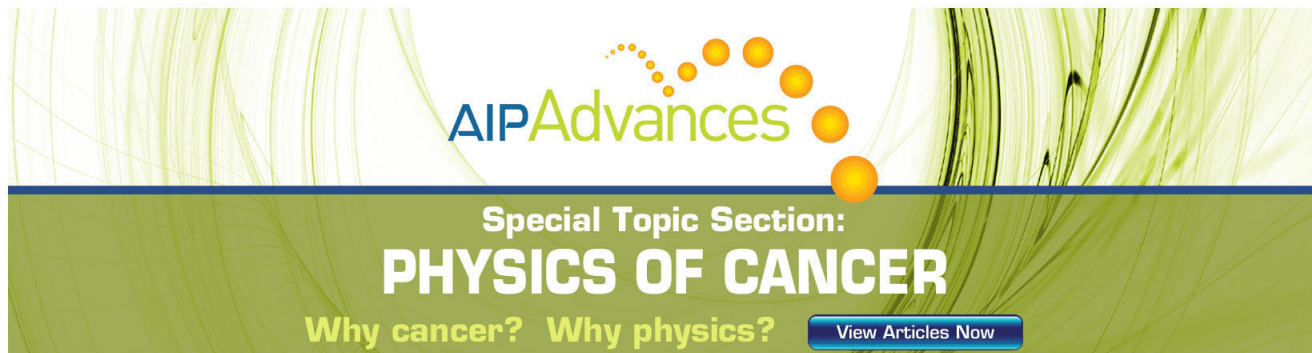
Journal Homepage: <http://apl.aip.org/>

Journal Information: [http://apl.aip.org/about/about\\_the\\_journal](http://apl.aip.org/about/about_the_journal)

Top downloads: [http://apl.aip.org/features/most\\_downloaded](http://apl.aip.org/features/most_downloaded)

Information for Authors: <http://apl.aip.org/authors>

## ADVERTISEMENT

The advertisement features a green and white background with abstract, flowing lines. At the top, the 'AIP Advances' logo is displayed, with 'AIP' in blue and 'Advances' in green, accompanied by a series of orange and yellow dots. Below the logo, the text 'Special Topic Section: PHYSICS OF CANCER' is written in white, with 'PHYSICS OF CANCER' in a larger, bold font. At the bottom, the phrase 'Why cancer? Why physics?' is written in green, and a blue button with the text 'View Articles Now' is positioned on the right side.

AIP Advances

Special Topic Section:  
**PHYSICS OF CANCER**

Why cancer? Why physics? [View Articles Now](#)

## Surface spin disorder and exchange-bias in hollow maghemite nanoparticles

Hafsa Khurshid,<sup>1,2,a)</sup> Wanfeng Li,<sup>2</sup> Manh-Huong Phan,<sup>1,a)</sup> Pritish Mukherjee,<sup>1</sup> George C. Hadjipanayis,<sup>2</sup> and Hariharan Srikanth<sup>1,a)</sup>

<sup>1</sup>Department of Physics, University of South Florida, Tampa, Florida 33620, USA

<sup>2</sup>Department of Physics and Astronomy, University of Delaware, Newark, Delaware 19716, USA

(Received 28 April 2012; accepted 16 June 2012; published online 9 July 2012)

We report a comparative study of the magnetic properties of polycrystalline hollow  $\gamma$ -Fe<sub>2</sub>O<sub>3</sub> nanoparticles with two distinctly different average sizes of  $9.2 \pm 1.1$  nm and  $18.7 \pm 1.5$  nm. High-resolution transmission electron microscopy images reveal the presence of a shell with thickness of 2 nm and 4.5 nm for the 9.2 nm and 18.7 nm nanoparticles, respectively. The field-cooled hysteresis loops show interesting features of enhanced coercivity and horizontal and vertical shifts associated with the polarity of the cooling field for both types of nanoparticles. While the anomalously large horizontal shifts and open hysteresis loop in a field as high as 9 T observed for the 9.2 nm nanoparticles corresponds to a “minor loop” of the hysteresis loop, the loop shift observed for the 18.7 nm nanoparticles manifests an intrinsic “exchange bias” (EB). Relative to the  $18.5 \pm 3.2$  nm solid nanoparticles, a much stronger EB effect is achieved in the 18.7 nm hollow nanoparticles. Our studies point to the importance of inner and outer surface spin disorder giving rise to surface anisotropy and EB and reveal a perspective of tuning EB in hollow magnetic nanoparticle systems. © 2012 American Institute of Physics. [<http://dx.doi.org/10.1063/1.4733621>]

Exchange bias (EB) in magnetic nanostructures is a topic of great current interest.<sup>1–5</sup> Several groups have focused on anomalous magnetic behavior in ferrite nanoparticles induced by surface spin disorder such as hysteresis loops exhibiting EB and high field irreversibility.<sup>6–14</sup> An explanation for this behavior is that when a large enough fraction of atoms reside at the surface of a particle, the broken exchange bonds are sufficient to induce surface spin disorder thus creating a core-shell structure made of the ferrite core with a shell of disordered spins.<sup>2,6</sup> These disordered spins can take on a number of configurations, one of which can be chosen by field-cooling the particle to induce an EB effect. It is thought that the lowest energy configuration of surface spins in the zero-field cooled condition of a spherical particle is the one in which the spins point in the radial direction from the particle.<sup>6,10</sup> The energy required to rotate these spins contributes to the enhanced coercivity below the spin freezing temperature as well as “open,” irreversible hysteresis up to high fields.<sup>6,7,9</sup> Although experimental studies have provided some evidences of surface spin disorder in fine particle systems,<sup>6,10</sup> the origin of the surface spin configuration remains under discussion.<sup>2,11,13</sup>

Recently, attention has been paid to an interesting class of hollow nanoparticles, which are composed of randomly oriented grains clumped together to form a hollow sphere.<sup>14–19</sup> These nanoparticles have potential applications in memristors, hyperthermia agent in nanomedicine, and targeted drug delivery.<sup>14</sup> The hollow nanoparticles are often synthesized utilizing the Kirkendall effect, which is associated with the difference in the diffusivities of atoms at the interface of two different materials causing supersaturation of lattice vacancies.<sup>20</sup> Since both inner and outer surfaces of a hollow nanoparticle contribute to enhance its total surface

area, this type of nanoparticle usually exhibits very high surface anisotropy  $K_s$ , which contributes to the effective anisotropy ( $K_{eff}$ ) of the whole system via  $K_{eff} = K_c + 6K_s/D$ , where  $K_c$  is the anisotropy associated with the core spins and  $D$  is the mean diameter of the nanoparticle. Jaffari *et al.*<sup>14</sup> showed that relative to a solid nanoparticle of NiFe<sub>2</sub>O<sub>4</sub> (the diameter of  $\sim 8$  nm), a hollow nanoparticle (the diameter of  $\sim 8$  nm and the shell thickness of  $\sim 2$  nm) possessed an increased surface area giving rise to enhanced spin disorder, surface anisotropy, and EB. Cabot *et al.*<sup>16</sup> also reported that owing to their high surface anisotropy,  $\gamma$ -Fe<sub>2</sub>O<sub>3</sub> hollow nanoparticles (the diameter of  $\sim 8.1$  nm and the shell thickness of  $\sim 1.6$  nm) exhibited small magnetization, large coercivity, and no magnetic saturation on external magnetic fields up to 5 T. While a very strong shift of the hysteresis loop, over 0.3 T, was observed for the  $\gamma$ -Fe<sub>2</sub>O<sub>3</sub> hollow nanoparticles when cooling the particles in a field of 5 T, this observed loop shift was attributed to the “minor loop” phenomenon,<sup>16</sup> rather than an EB effect.<sup>18</sup> Interestingly, their Monte Carlo simulation study predicts that if the number of surface spins increases, the low-temperature magnetic behavior would be dominated by the crystallographic anisotropy.<sup>16</sup> All this raises up a very fundamental and important question: Can one tune “minor loop” to “exchange bias” effects in  $\gamma$ -Fe<sub>2</sub>O<sub>3</sub> hollow nanoparticles by varying the number of surface spins (the thickness of the shell)?

To address this emerging question, we have performed a comparative study of  $\gamma$ -Fe<sub>2</sub>O<sub>3</sub> hollow nanoparticles with two distinct different sizes of  $9.2 \pm 1.1$  nm (the shell thickness of  $\sim 2$  nm) and  $18.7 \pm 1.5$  nm (the shell thickness of  $\sim 4.5$  nm). In addition to the “minor loop” behavior observed for the 9.2 nm hollow nanoparticles, similar to the case of Cabot *et al.*,<sup>16</sup> we have observed an *intrinsic* EB effect in the 18.7 nm hollow nanoparticles. As compared with the  $18.5 \pm 3.2$  nm solid  $\gamma$ -Fe<sub>2</sub>O<sub>3</sub> nanoparticles, a large enhancement of the EB in the 18.7 nm hollow  $\gamma$ -Fe<sub>2</sub>O<sub>3</sub> nanoparticles

<sup>a)</sup>Authors to whom correspondence should be addressed. Electronic addresses: hkhurshi@usf.edu, phanm@usf.edu, and sharihar@usf.edu.

is found to be associated with the presence of the inner surface spins. Our studies demonstrate, the possibility of tuning “minor loop” to “exchange bias” effects in  $\gamma$ -Fe<sub>2</sub>O<sub>3</sub> hollow nanoparticle systems by varying the number of surface spins (varying the shell thickness of the hollow nanoparticles). This is of practical importance as such nanostructures can be ideal for use in applications where their anisotropic magnetic properties can be controlled using the so-called “exchange bias” mechanism.<sup>5,19</sup>

A detailed description of the synthesis of  $\gamma$ -Fe<sub>2</sub>O<sub>3</sub> hollow nanoparticles that we have studied in the present work was reported elsewhere.<sup>21</sup> Briefly, thermal decomposition of iron pentacarbonyl at high temperature in air-free environment is employed to produce core/shell structured iron/iron-oxide nanoparticles. The hollow nanoparticles were produced by further oxidizing the core/shell nanoparticles which became hollow via the so-called Kirkendall effect. Figure 1 shows transmission electron microscopy (TEM) and high-resolution TEM images of the synthesized hollow nanoparticles. A representative graph of the histogram of the particle sized populations as observed from the TEM image is also included in the inset of Fig. 1(a). From a histogram analysis of the TEM images, the average particle size is estimated to be  $9.2 \pm 1.1$  nm and  $18.7 \pm 1.5$  nm for the two synthesized hollow nanoparticle samples. These size distributions are also checked to be consistent with the observed blocking temperatures in the dc magnetic characterizations. The high-resolution TEM images clearly show that these hollow nanostructures are composed of randomly oriented grains

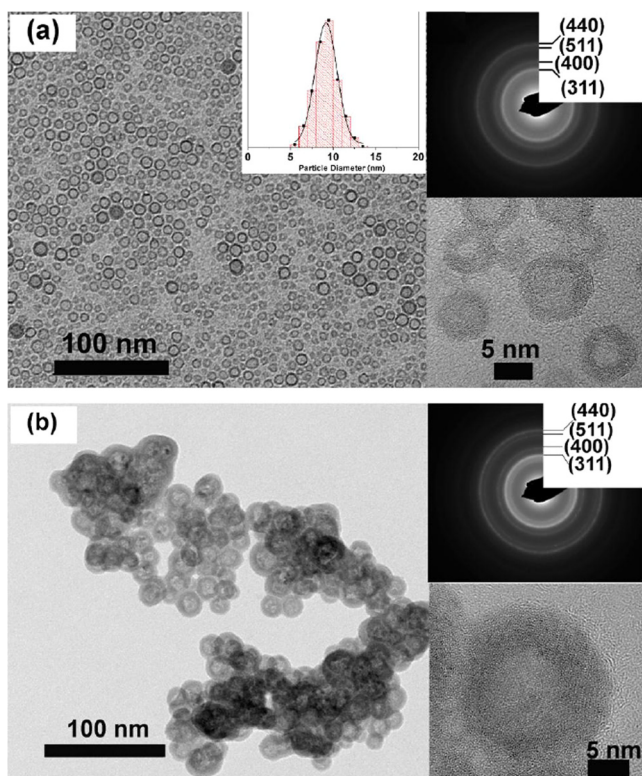


FIG. 1. Bright field TEM images of (a) 9.2 nm and (b) 18.7 nm hollow nanoparticles along with the size distribution and SAD corresponding to iron oxide and HRTEM. The histogram of the particle sized populations as observed from the TEM image of the 9.2 nm hollow nanoparticle sample is also included in the inset of (a).

that stick together to make a hollow shell. The shell thicknesses of the 9.2 nm and 18.7 nm particles are determined to be about 2 nm and 4.5 nm, respectively.

The magnetic properties of the synthesized hollow nanoparticles were measured using a commercial Physical Properties Measurement System (PPMS) from Quantum Design. Figure 2 shows the temperature dependence of zero-field-cooled (ZFC) and field-cooled (FC) magnetization for the 9.2 nm and 18.7 nm hollow nanoparticles at an applied field of 10 mT. We have observed that the overall shape of the FC and ZFC curves of the 9.2 nm hollow nanoparticles with a shell thickness of 2 nm is similar to that reported by Cabot *et al.*<sup>16</sup> for the 8.1 nm hollow nanoparticles with a shell thickness of 1.6 nm and by Schevchenko *et al.*<sup>18</sup> for the 11 nm hollow nanoparticles with a shell thickness of 2 nm. The temperature at the ZFC peak, often defined as the blocking temperature ( $T_B$ ), is determined to be about 60 K for the 9.2 nm hollow nanoparticles. This value of  $T_B$  is smaller than that of the 11 nm hollow nanoparticles ( $T_B \sim 65$  K)<sup>18</sup> but larger than that of the 8.1 nm hollow nanoparticles ( $T_B \sim 34$  K).<sup>16</sup> Noticeably, this value is much higher than that of the 7 nm solid maghemite nanoparticles having a similar particle volume ( $T_B \sim 20$  K) reported by Shendruk *et al.*<sup>10</sup> This has been attributed to the enhanced anisotropy energy and/or magnetic interactions among domains within each hollow particle.<sup>16,19</sup> Using the crystallite size determined from the TEM image (Fig. 1) and the experimentally observed value of  $T_B$  (Fig. 2), we have quantitatively estimated the magnetic anisotropy energy from the standard expression,  $K_{eff}V = 25k_B T_B$ , where  $K_{eff}$  is the effective anisotropy,  $V$  is the particle volume, and  $k_B$  the Boltzmann constant. For the 9.2 nm hollow particles with a 2 nm thick shell, the estimated value of  $K_{eff}$  is  $7.1 \times 10^7$  erg/cc, which is about two orders of magnitude larger than that of the 7 nm solid nanoparticles<sup>10</sup> ( $K_{eff} \sim 1.2 \times 10^5$  erg/cc) and is three orders of magnitude larger than that of bulk maghemite<sup>22</sup> ( $K_{eff} \sim 4.7 \times 10^4$  erg/cc). This can be understood by considering the fact that in the case of small nanoparticles, the atoms/spins lying at or near the surface could cause a great enhancement of the surface anisotropy, magnetic frustration, and spin disorder. Spin canting at the surface ions of ferrite magnetic nanoparticles has been revealed by Mossbauer

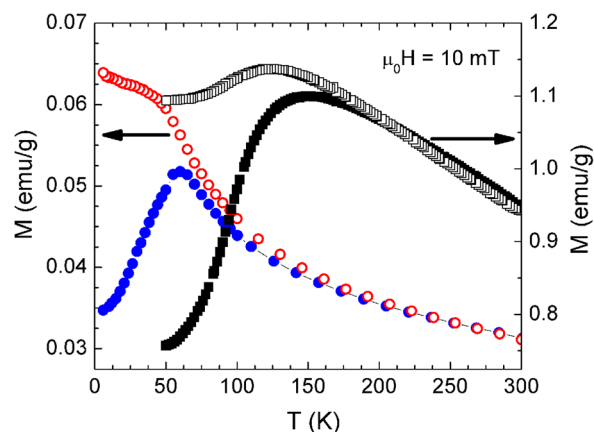


FIG. 2. The zero-field-cooled (solid symbols) and field-cooled (open symbols) magnetization versus temperature  $M(T)$  curves for 9.2 nm (spheres) and 18.7 nm (squares) hollow nanoparticles at an applied field of 10 mT.

spectra in applied fields.<sup>23</sup> The surface effects are even more pronounced for the hollow nanoparticles due to the availability of extra surface layers (inner layer) and at the interface between randomly oriented grains in the shell. Thus, the large particle anisotropy obtained for the hollow nanoparticles can be attributed to the enhanced contribution from both surface and finite size effects.<sup>2,16</sup>

For the case of the 18.7 nm hollow particles with a 4.5 nm thick shell, the obtained value of  $T_B$  is 150 K, which is much larger than that of the 9.2 nm hollow particles with a 2 nm thick shell ( $T_B \sim 60$  K). However, the value of  $K_{eff}$  estimated for the 18.7 nm hollow particles with a 4.5 nm thick shell ( $8.5 \times 10^6$  erg/cc) is smaller than that of the 9.2 nm hollow particles with a 2 nm thick shell ( $7.1 \times 10^7$  erg/cc). This suggests a larger number of disordered surface spins in the 9.2 nm hollow particles than in the 18.7 nm hollow particles. This hypothesis is supported by considering the difference in the surface to volume ratios of the two sizes. The 9.2 nm hollow nanoparticles have the surface to volume ratio of 0.56, which is about twice higher than that of the 18.7 nm hollow particles (0.28). This is also reconciled with the room temperature and low temperature  $M(H)$  data that show a non-saturated magnetization behavior for the 9.2 nm hollow particles (Fig. 3(a)), in contrast to the 18.7 nm hollow particles (Fig. 3(b)). The 18.7 nm hollow particles have a room temperature maximum magnetization of 22.1 emu/g that increases to 24.7 emu/g at 50 K, whereas the 9.2 nm hollow nanoparticles have a room temperature maximum magnetization of only 1.2 emu/g that increases to 3.8 emu/g at 50 K. These values of magnetization are much lower than that of

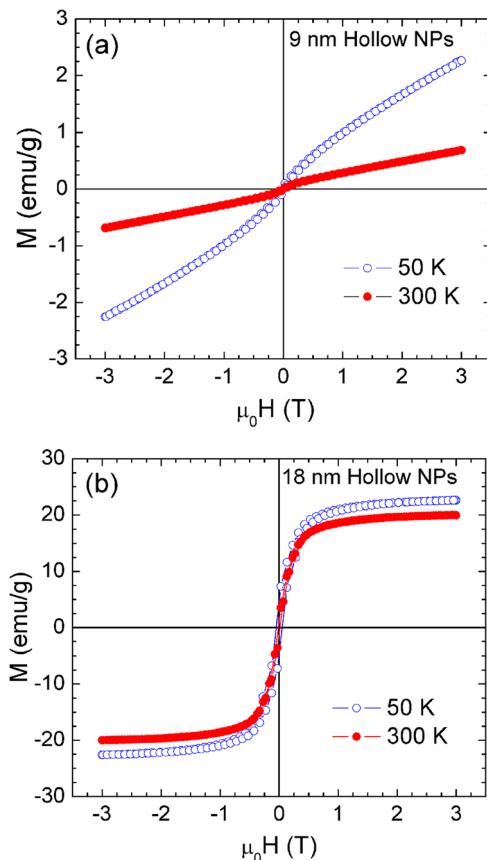


FIG. 3. The magnetic hysteresis  $M(H)$  loops taken at 300 K and 50 K for the 9.2 nm (a) and 18.7 nm (b) hollow nanoparticles.

bulk  $\gamma\text{-Fe}_2\text{O}_3$  ( $\sim 80$  emu/g),<sup>22</sup> giving a clear indication of the high magnetic frustration and high fraction of surface spins present in the hollow particles. A monotonic increase in magnetization with respect to the applied magnetic field for both loops taken at 300 K and 50 K (Fig. 3(a)) clearly indicates a larger contribution from paramagnetic susceptibility in the case of the 9.2 nm hollow particles.

In order to quantify the superparamagnetic (SPM) and paramagnetic (PM) contributions to the magnetic moment, the experimental  $M(H)$  data were fitted to the Langevin function with an added linear term (Eq. (1)) to extract the paramagnetic contribution to the magnetization

$$M(H) = M_S^{SPM} \left[ \coth\left(\frac{\mu H}{KT}\right) - \left(\frac{\mu H}{KT}\right)^{-1} \right] + C^{PM}H, \quad (1)$$

where  $M_S^{SPM}$  is the saturation magnetization of the SPM part and  $\mu$  is the average magnetic moment of SPM particles.  $C^{PM}$  is the susceptibility of the paramagnetic contribution that is linear with the magnetic field  $H$ . The experimental data and fitted curves are displayed in Figs. 4(a) and 4(b) for both types of hollow particles. It can be seen that for the case of the 9.2 nm hollow nanoparticles, SPM susceptibility contributes to only 13% of the total magnetic moment, while the rest of it (87%) comes from the paramagnetic susceptibility. For the case of the 18.7 nm hollow nanoparticles, however,

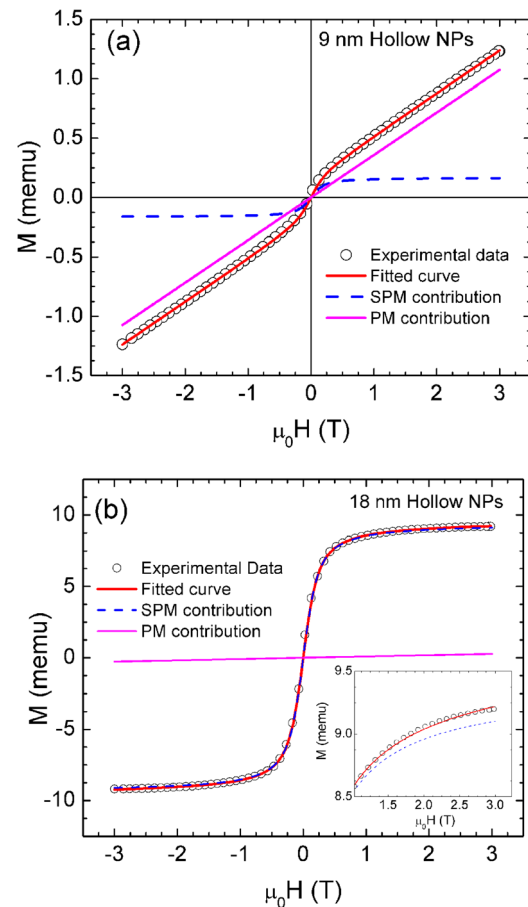


FIG. 4. The  $M(H)$  curves at 300 K are fitted (red) to Eq. (1); the blue and magenta (dashed) curves represent the simulated SPM and PM contributions extracted from the experimental data using the fitting parameters for the 9.2 nm (a) and 18.7 nm (b) hollow nanoparticles.

SPM susceptibility contributes 97% to the total magnetic moment and the only 3% contribution comes from the PM susceptibility. Since a highly linear contribution to the magnetization results mainly from the uncompensated spins at the shell surfaces and crystallite interfaces, these results once again suggest a larger number of disordered surface spins present in the 9.2 nm hollow particles than in the 18.7 nm hollow particles.<sup>16</sup> This can quantitatively explain the non-saturation feature of magnetization and the smaller value of magnetization for the 9.2 nm hollow particles, as compared to the 18.7 nm hollow particles.

As we discussed above, as a consequence of broken exchange bonds and lower crystal symmetry, spins near the surface of a nanoparticle are highly disordered and the layer of these disordered surface spins may enter a spin-glass-like state at a low temperature below which a shift in the hysteresis loop (the so-called exchange bias) is often observed as the particle system is cooled from a temperature above  $T_B$  in the presence of a magnetic field. It has been reported that 7 nm solid  $\gamma$ -Fe<sub>2</sub>O<sub>3</sub> nanoparticles undergo a spin-glass-like transition at  $\sim 15$  K below which the surface anisotropy sharply increases and EB occurs resulting from a strong exchange coupling between the shell of disordered spins and the core of ordered spins.<sup>10</sup> To investigate these effects in the present hollow nanoparticles, both samples (the 9.2 nm and 18.7 nm hollow particles) were cooled from 300 K down to low temperatures in different magnetic fields. As shown in Fig. 5(a), the unusually large horizontal and vertical shifts in

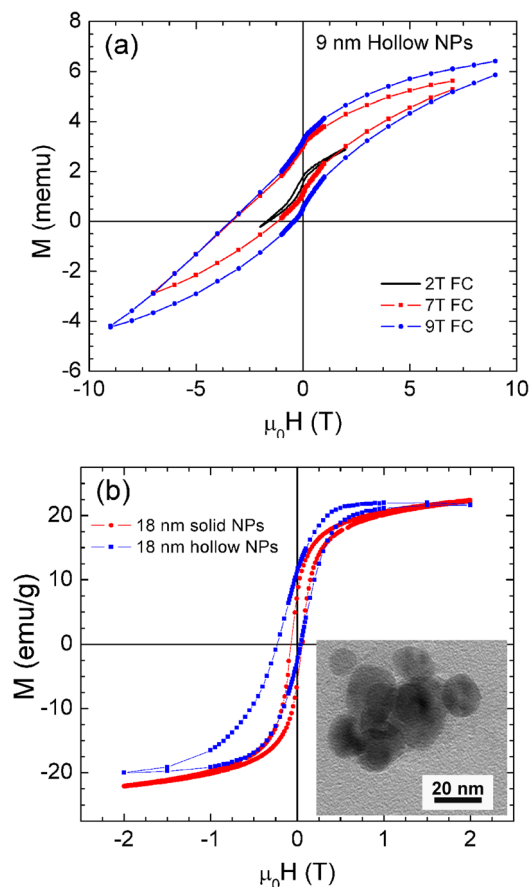


FIG. 5. The FC  $M(H)$  loops taken at 5 K for (a) 9.2 nm and (b) 18.7 nm hollow nanoparticles. The TEM image of the 18.5 nm solid nanoparticles is shown in the inset of (b).

the  $M(H)$  loops occur for the 9.2 nm hollow particles in a cooling field as high as 9 T. Due to their very high anisotropy field, the  $M(H)$  loops are not closed as the maximum applied field was not sufficient to saturate the magnetization of the sample. As a result, the obtained values of coercive field ( $H_c$ ) might not be a true representation of the intrinsic coercivity.<sup>24</sup> Similar behavior was also observed for the 8.1 nm hollow  $\gamma$ -Fe<sub>2</sub>O<sub>3</sub> particles.<sup>16</sup> In both cases, since the maximum applied field is lower than the irreversibility field, the observed loop shift must correspond to a minor loop of the hysteresis loop, rather than an EB phenomenon. As compared with the 7 nm solid  $\gamma$ -Fe<sub>2</sub>O<sub>3</sub> particles,<sup>10</sup> a much stronger loop shift has been observed for the 9.2 nm hollow particles in our study and for the 8.1 nm hollow particles by Cabot *et al.*<sup>16</sup> and for the 11 nm hollow particles by Schevchenko *et al.*<sup>18</sup> This can be attributed to a larger portion of disordered spins locating at the innermost or outermost surfaces of the shell and at the interfaces between crystallographic domains. It is very interesting to note that unlike the case of the 9.2 nm hollow particles, the loop shift observed for the 18.7 nm hollow particles represents an *intrinsic* EB effect. For this sample, the EB field  $H_E$  is calculated to be about 96 mT and the coercive field  $H_c$  is 1.36 T at 5 K. This value of  $H_E$  is about 35 times larger than that of the 7 nm solid  $\gamma$ -Fe<sub>2</sub>O<sub>3</sub> particles ( $H_E \sim 2.7$  mT at 5 K in a field of 2.5 T).<sup>10</sup> These results clearly point to the important role of inner and outer surface spins in enhancing the observed EB effect in the hollow nanoparticles.

Although the presence of inner surface spins is believed to play an important role in enhancing the EB in  $\gamma$ -Fe<sub>2</sub>O<sub>3</sub> hollow nanoparticles, no experimental work has been made to verify this hypothesis. Therefore, in the present work we attempt to elucidate this through a comparative study of the EB effect in two types of nanoparticles: the 18.5 nm  $\gamma$ -Fe<sub>2</sub>O<sub>3</sub> solid nanoparticles and the 18.7 nm  $\gamma$ -Fe<sub>2</sub>O<sub>3</sub> hollow nanoparticles. The  $18.5 \pm 3.2$  nm solid nanoparticles were synthesized by annealing their corresponding hollow nanoparticles.<sup>14</sup> These particles have a relatively broad size distribution due to the fact that particles annealed in the form of the dried powder particles could be agglomerated to some extent. A representative TEM image of this sample is shown in the inset of Fig. 5(b). Having assumed an equal number of outer surface spins for both types of particles, one would expect that due to the absence of inner surface spins, the 18.5 nm solid nanoparticles should show a smaller EB effect as compared to the 18.7 nm hollow nanoparticles. As shown in Fig. 5(b), for the same cooling field of 2 T, at 5 K the EB field of the 18.5 nm solid nanoparticles ( $H_E \sim 14$  mT) is about 7 times smaller than that of the 18.7 nm hollow nanoparticles ( $H_E \sim 96$  mT). This result clearly points to the important role of inner surface spins in enhancing the EB effect in the  $\gamma$ -Fe<sub>2</sub>O<sub>3</sub> hollow nanoparticles. We note that the Monte Carlo simulation study shows that the magnetic exchange interactions between spins with different crystallographic easy axis inside the shell have a noticeable but not dominant influence on the hysteresis loops.<sup>16</sup>

In summary, we have studied the magnetic properties of  $\gamma$ -Fe<sub>2</sub>O<sub>3</sub> hollow nanoparticles with two distinct different sizes of  $9.2 \pm 1.1$  nm (the shell thickness of 2 nm) and  $18.7 \pm 1.5$  nm (the shell thickness of 4.5 nm). Our studies reveal that by varying the thickness of the shell (varying the

number of surface spins), it is possible to tune the anisotropic field and EB field in hollow nanoparticle systems. The origins of the strong anisotropy energy and exchange bias effect observed in these systems are associated with the large portion of disordered spins locating at the innermost or outermost surfaces of the shell and at the interfaces between crystallographic domains.

Research at UD was supported by National Science Foundation (DMR0302544). Research at USF was supported by the Center for Integrated Functional Materials through grant USAMRMC W81XWH-10-2-0101. MHP thanks the support from the Florida Cluster for Advanced Smart Sensor Technologies. The authors would like to thank Dr. A. M. Gabay and R. Schmidt for their helpful discussions and technical assistance with some magnetic measurements.

- <sup>1</sup>J. Nogués, J. Sort, V. Langlais, V. Skumryev, S. Suriñach, S. S. Muñoz, and M. D. Baró, *Phys. Rep.* **422**, 65 (2005).
- <sup>2</sup>O. Iglesias, A. Labarta, and X. Batlle, *J. Nanosci. Nanotech.* **8**, 2761 (2008).
- <sup>3</sup>S. Giri, M. Patra, and S. Majumdar, *J. Phys.: Condens. Matter* **23**, 073201 (2011).
- <sup>4</sup>S. Laureti, S. Y. Suck, H. Haas, E. Prestat, O. Bourgeois, and D. Givord, *Phys. Rev. Lett.* **108**, 077205 (2012).
- <sup>5</sup>X. L. Sun, N. F. Huls, A. Sigdel, and S. S. Sun, *Nano Lett.* **12**, 246 (2012).
- <sup>6</sup>R. H. Kodama, A. E. Berkowitz, E. J. McNiff, Jr., and S. Foner, *Phys. Rev. Lett.* **77**, 394 (1996).
- <sup>7</sup>B. Martinez, X. Obradors, L. Balcells, A. Rouanet, and C. Monty, *Phys. Rev. Lett.* **80**, 181 (1998).

- <sup>8</sup>R. K. Zheng, G. H. Wen, K. K. Fung, and X. X. Zhang, *Phys. Rev. B* **69**, 214431 (2004).
- <sup>9</sup>H. Wang, T. Zhu, K. Zhao, W. N. Wang, C. S. Wang, Y. J. Wang, and W. S. Zhan, *Phys. Rev. B* **70**, 092409 (2004).
- <sup>10</sup>T. N. Shendruk, R. D. Desautels, B. W. Southern, and J. van Lierop, *Nanotechnology* **18**, 455704 (2007).
- <sup>11</sup>D. Peddos, C. Cannas, G. Piccaluga, E. Agostinelli, and D. Fiorani, *Nanotechnology* **21**, 125705 (2010).
- <sup>12</sup>J. Sánchez-Marcos, M. A. Laguna-Marco, R. Martínez-Morillas, E. Céspedes, F. Jiménez-Villacorta, N. Menéndez, and C. Prieto, *J. Phys. Condens. Matter* **23**, 476003 (2011).
- <sup>13</sup>Y. Hwang, S. Angappane, J. Park, K. An, T. Hyeon, and J. G. Park, *Curr. Appl. Phys.* **12**, 808 (2012).
- <sup>14</sup>G. H. Jaffari, A. Ceylan, C. Ni, and S. I. Shah, *J. Appl. Phys.* **107**, 013910 (2010).
- <sup>15</sup>Q. K. Ong, A. Wei, and X. M. Lin, *Phys. Rev. B* **80**, 134418 (2009).
- <sup>16</sup>A. Cabot, A. P. Alivisatos, V. F. Puentes, L. Balcells, O. Iglesias, and A. Labarta, *Phys. Rev. B* **79**, 094419 (2009).
- <sup>17</sup>Q. K. Ong, X. M. Min, and A. Wei, *J. Phys. Chem. C* **115**, 2665 (2011).
- <sup>18</sup>E. V. Schevchenko, M. I. Bodnarchuk, M. V. Kovalenko, D. V. Talapin, R. K. Smith, S. Aloni, W. Heiss, and A. P. Alivisatos, *Adv. Mater.* **20**, 4323 (2008).
- <sup>19</sup>K. Simeonidis, C. Martinez-Boubeta, O. Iglesias, A. Cabot, M. Angelakeris, S. Mourdikoudis, I. Tsiaoussis, A. Delimitis, C. Dendrinou-Samara, and O. Kalogirou, *Phys. Rev. B* **84**, 144430 (2011).
- <sup>20</sup>H. J. Fan, U. Gçsele, and M. Zacharias, *Small* **3**, 1660 (2007).
- <sup>21</sup>H. Khurshid, V. Tzitzios, F. Li, and G. C. Hadjipanayis, *Nanotechnology* **22**, 265605 (2011).
- <sup>22</sup>J. M. D. Coey, *Phys. Rev. Lett.* **27**, 1140 (1971).
- <sup>23</sup>C. R. Alves, R. Aquino, J. Depeyrot, T. A. P. Cotta, M. H. Sousa, F. A. Tourinho, H. R. Rechenberg, and G. F. Goya, *J. Appl. Phys.* **99**, 08M905 (2006).
- <sup>24</sup>H. M. Nguyen and P.-Y. Hsiao, *Appl. Phys. Lett.* **94**, 186101 (2009).